JOURNAL OF GUIDANCE, CONTROL, AND DYNAMICS
Vol. 32, No. 5, September–October 2009

Engineering Notes

Robust Control Moment Gyroscope Steering Logic with Gimbal Angle Constraints

V. Lappas*
University of Surrey,
Guildford, Surrey GU2 7XH, United Kingdom
and
B. Wie†
Iowa State University, Ames, Iowa 50011

DOI: 10.2514/1.43806

Introduction

SINGLE gimbal control moment gyroscopes are constant speed momentum wheels, gimbaled in one axis only. For full three-axis control of a spacecraft, a cluster of four control moment gyroscopes (CMGs) is normally used. CMGs, due to their inherit gyroscopic properties can potentially generate large torque and angular momentum outputs, in a more efficient way than current technologies, such as reaction or momentum wheels. Depending on the gimbal axes, a CMG can be distinguished to a single gimbal CMG (SGCMG) and double gimbal CMG (DGCMG). The type and number of CMGs that can be used in an attitude control system are a tradeoff between performance, cost, mechanical, and algorithm complexity. SGCMGs (referred to as CMGs in this work) are mainly considered in this Note. CMGs have been thoroughly studied in the past and have been baselined to be used in future space missions [1–3]. The most important drawback of CMGs is the singularity problem. CMGs encounter singular states where, for a particular gimbal angle geometric configuration, they cannot produce control torque along a certain direction. There have been many singularity avoidance logics that mitigate this problem, with different advantages and disadvantages [1–4]. This Note extends current work on singularity avoidance when a gimbal angle constraint is imposed.

Problem Formulation

CMGs are mechanically complex devices. Using flywheels at a continuous high spin rate (∼5000 rpm) and gimbal systems with high spin rates (∼30–90 deg/s) can become susceptible to lifetime failures when used intensely. A miniature CMG developed at the University of Surrey is a low-cost approach toward giving small satellites an agile capability [1,3]. However, the CMG has been designed with a mechanical stop that does not allow a full 360 deg rotation but constrains the gimbal angle to ±180 deg, as depicted in Fig. 1. This design was deemed to be the quickest, low-cost, and least complex solution for developing the CMGs in time for the BILSAT-1 launch [1]. Although the BILSAT-1 twin CMG cluster is used as an experimental payload, using these units in a four-CMG cluster in pyramid configuration on a future satellite poses the problem of being able to escape all types of singularities while coping with a

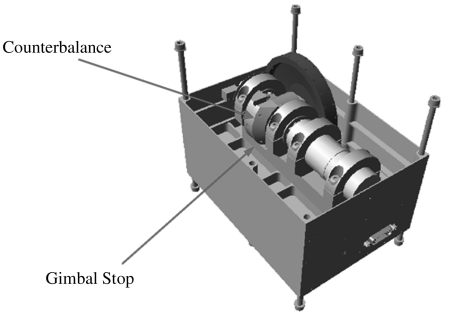

Fig. 1 BILSAT-1 CMG model.

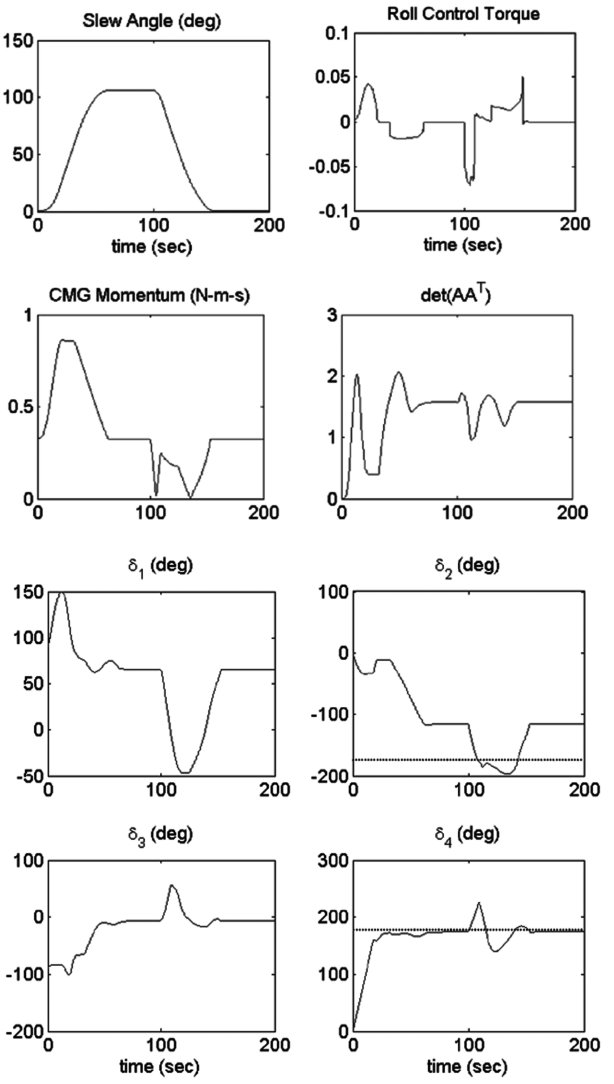

Fig. 2 Roll rest-to-rest maneuver without gimbal constraint.

Presented as Paper 6651 at the AIAA/AAS Astrodynamics Specialist Conference and Exhibit, Keystone, CO, 21–24 August 2006; received 13 February 2009; revision received 26 May 2009; accepted for publication 27 May 2009.

*Senior Lecturer, Surrey Space Center. Senior Member AIAA.
†Vance Coffman Endowed Chair Professor, Department of Aerospace Engineering. Associate Fellow AIAA.

Table 1 Simulation parameters

Parameter	Value	Units
h_0	0.28	Nm
$\mathbf{I}_{xx}, \mathbf{I}_{yy}, \mathbf{I}_{zz}$	[10, 10, 10]	kg · m^2
β	54.73	deg
$\lvert\omega_i\rvert_{\max}$	6	deg /s
$\dot{\delta}_{\max}$	12	deg /s
$\boldsymbol{\delta}^*$	±180	deg
$\boldsymbol{\delta}_i$	[90, 0, −90, 0]	deg
γ	0.01	——

hardware constraint of a ±180 deg gimbal constraint. The use of the novel steering logic with a gimbal angle constraint for micro-CMGs can significantly reduce the cost and complexity of a CMG design and can increase design robustness against possible failures due to the use of slip rings in the CMG gimbal mechanism. This Note shows that there are cases in which a singularity occurs which requires gimbal angles to diverge to values that exceed the ±180 deg gimbal constraint. The gimbal angle constraint will require a new modified steering logic that will permit transition through a singularity while meeting all hardware constraints. The classical four-CMG cluster is used with a skew angle β of 54.73 deg, as discussed in [3–5]. The CMG parameters are presented in Table 1. The rotational equation of motion for spacecraft with CMGs for a spacecraft with momentum exchange devices is given by

$$\dot{\mathbf{H}}_s + \boldsymbol{\omega} \times \mathbf{H}_s = \mathbf{N}_{\text{ext}} \tag{1}$$

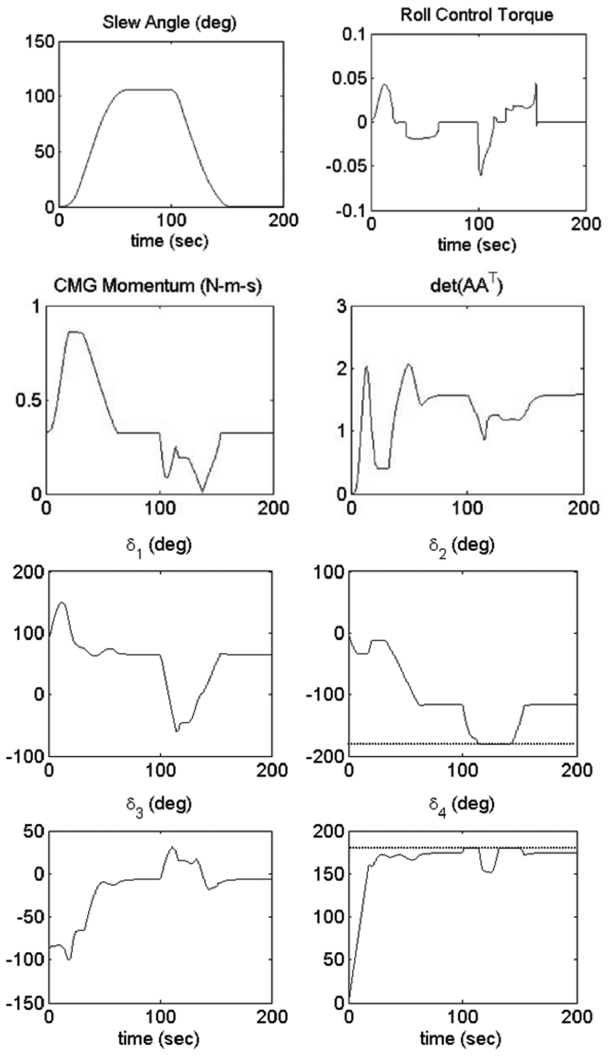

Fig. 3 Roll rest-to-rest maneuver with gimbal constraint.

where $\mathbf{H}_s$ is the angular momentum vector relative to the inertial frame which is expressed in the body-fixed frame, and $\mathbf{N}_{\text{ext}}$ is the external torque vector, including all types of external disturbances. The total angular momentum is given by

$$\mathbf{H}_s = \mathbf{I}\boldsymbol{\omega} + \mathbf{h} \tag{2}$$

where $\mathbf{I}$ is the spacecraft inertia matrix, $\boldsymbol{\omega}$ is the angular velocity vector, and $\mathbf{h}$ is the total CMG momentum vector. The total CMG angular momentum vector $\mathbf{h} = [h_x, h_y, h_z]^T$ is expressed with respect to the spacecraft reference frame as

$$\mathbf{h} = \sum_{i=1}^{4} \mathbf{H}_i(\delta_i) \tag{3}$$

$$\mathbf{h} = \sum_{i=1}^{4} \mathbf{H}_i(\delta_i) = h_0 \begin{bmatrix} -c\beta \sin\delta_1 & -\cos\delta_2 & c\beta \sin\delta_3 & \cos\delta_4 \\ \cos\delta_1 & -c\beta \sin\delta_2 & -\cos\delta_3 & c\beta \sin\delta_4 \\ s\beta \sin\delta_1 & s\beta \sin\delta_2 & s\beta \sin\delta_3 & s\beta \sin\delta_4 \end{bmatrix} \tag{4}$$

where β is the pyramid skew angle, $c\beta = \cos\beta$, $s\beta = \sin\beta$, and δ_i are the gimbal angles, and h_0 is the magnitude of the angular momentum produced by the flywheel, of each CMG. Substitution of Eqs. (2–4) in Eq. (1) allows inversion and calculation of the gimbal rate commands using the pseudoinverse [3–6] as

$$\dot{\boldsymbol{\delta}} = \mathbf{A}^+\dot{\mathbf{h}} = \mathbf{A}^T(\mathbf{A}\mathbf{A}^T)^{-1}\dot{\mathbf{h}}$$

$$\mathbf{A} = \begin{bmatrix} -c\beta c\delta_1 & s\delta_2 & c\beta c\delta_3 & -s\delta_4 \\ -s\delta_1 & -c\beta c\delta_2 & s\delta_3 & c\beta c\delta_4 \\ s\beta c\delta_1 & s\beta c\delta_2 & s\beta c\delta_3 & s\beta c\delta_4 \end{bmatrix} \tag{5}$$

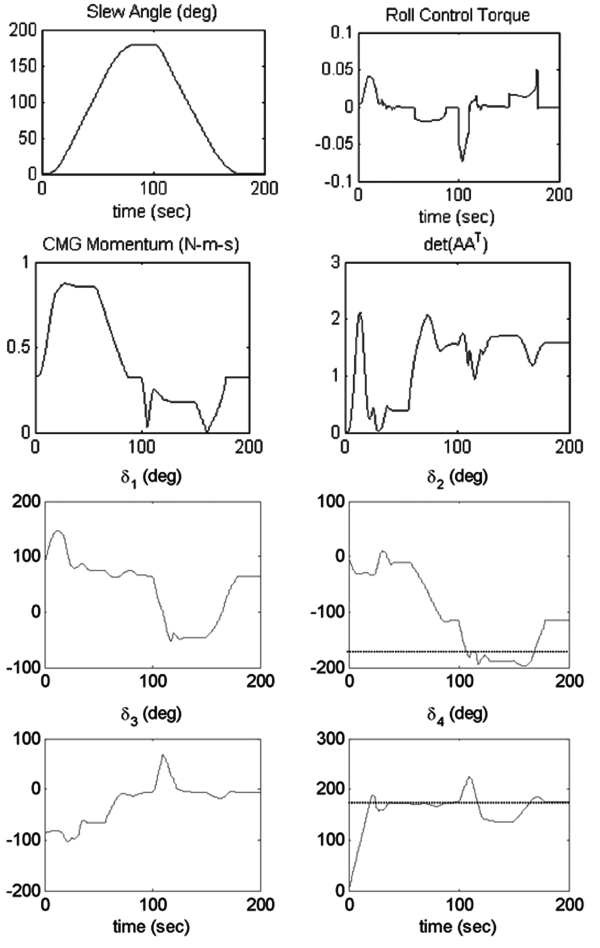

Fig. 4 Roll rest-to-rest 180 deg maneuver without gimbal constraint.

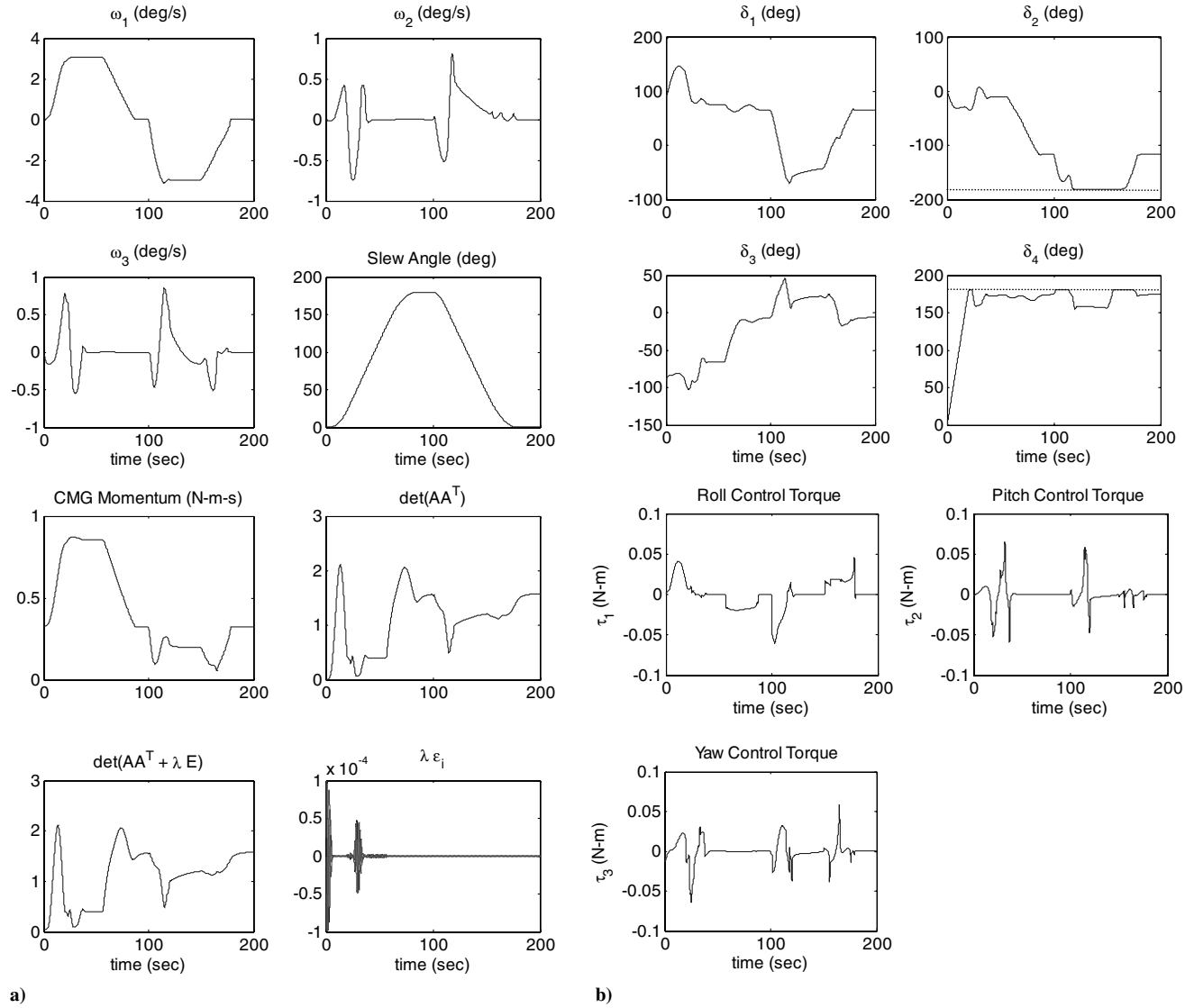

Fig. 5 Roll rest-to-rest 180 deg maneuver with gimbal constraint.

This Note does not focus on singularity avoidance or on the detailed mathematical description of the CMG cluster. The steering logic used in this Note is based on [5] in which the pseudoinverse is based on the generalized singularity robust law:

$$\mathbf{A}^{\#} = \mathbf{A}^T[\mathbf{A}\mathbf{A}^T + \lambda\mathbf{E}]^{-1} \qquad \mathbf{E} = \begin{bmatrix} 1 & \varepsilon_3 & \varepsilon_2 \\ \varepsilon_3 & 1 & \varepsilon_1 \\ \varepsilon_2 & \varepsilon_1 & 1 \end{bmatrix} \tag{6}$$

where $\varepsilon_i = \varepsilon_0 \sin(\omega t + \varphi_i)$ and ε_0 is the amplitude, ω is the frequency, and φ_i phases to be properly selected. For large slew angles, CMG systems are susceptible to encounter singularities. For a CMG system with a 180 deg gimbal constraint, this can be a problematic situation. Figure 2 shows a 106 deg roll rest-to-rest maneuver. If the worse case for a CMG system is used, that is, starting from an elliptic singularity ($[\delta_i = 90, \quad 0, \quad -90, \quad 0]$ deg), the gimbal angles diverge and would have to extend over the hard limit of ± 180 deg.

Gimbal Angle Constraint and Simulation Results

A CMG steering logic is proposed for a CMG system with gimbal angle constraints as follows:

$$\boldsymbol{\tau} = -\mathbf{J}\left\{2k\,\mathrm{sat}_{L_i}\left(\mathbf{e} + \frac{1}{T}\int \mathbf{e}\right) + c\boldsymbol{\omega}\right\} \tag{7a}$$

$$L_i = \frac{c}{2k}\min\left\{\sqrt{4a_i|e_i|}, |\omega_i|_{\max}\right\} \tag{7b}$$

$$\mathbf{A}^{\#} = \mathbf{A}^T[\mathbf{A}\mathbf{A}^T + \lambda\mathbf{E}]^{-1} \tag{7c}$$

$$\mathbf{u} = -\boldsymbol{\tau} - \boldsymbol{\omega} \times \mathbf{h} \tag{7d}$$

$$\dot{\boldsymbol{\delta}}_c = \mathrm{sat}_{\pm\dot{\delta}_{\max}}\{\mathbf{A}^{\#}\mathbf{u} + \gamma[\mathbf{I} - \mathbf{A}^{\#}\mathbf{A}](\boldsymbol{\delta}^* - \boldsymbol{\delta})\} \tag{7e}$$

$$\dot{\boldsymbol{\delta}}_{ci} = 0 \quad \text{when } |\delta_i| \geq \delta_{\max} \quad \text{and} \quad \mathrm{sgn}(\delta_i)\dot{\delta}_{ci} > 0 \tag{7f}$$

where $\dot{\delta}_{\max}$ is the maximum gimbal rate, $|\omega_i|_{\max}$ is the maximum slew rate, $\mathbf{u}$ is the control torque input, $\mathbf{J}$ is the spacecraft moment of inertia, $\mathbf{e}$ is the quaternion error vector, $\boldsymbol{\tau}$ is the internal control torque vector generated by the CMGs, $\boldsymbol{\delta}^*$ denotes a set of desired gimbal angles, and γ is a positive scalar. The test case selected is for an elliptic singularity ($[\delta_i = 90, \quad 0, \quad -90, \quad 0]$ deg), which demonstrates the escape logic capability of the system and simultaneously steering the gimbal angles away from the ± 180 deg constraint. Equations (7a–7d) are based on existing control logics derived and discussed in detail in [5,6]. Equation (7e) calculates the gimbal rate command for two different tasks: 1) the first part of the equation,

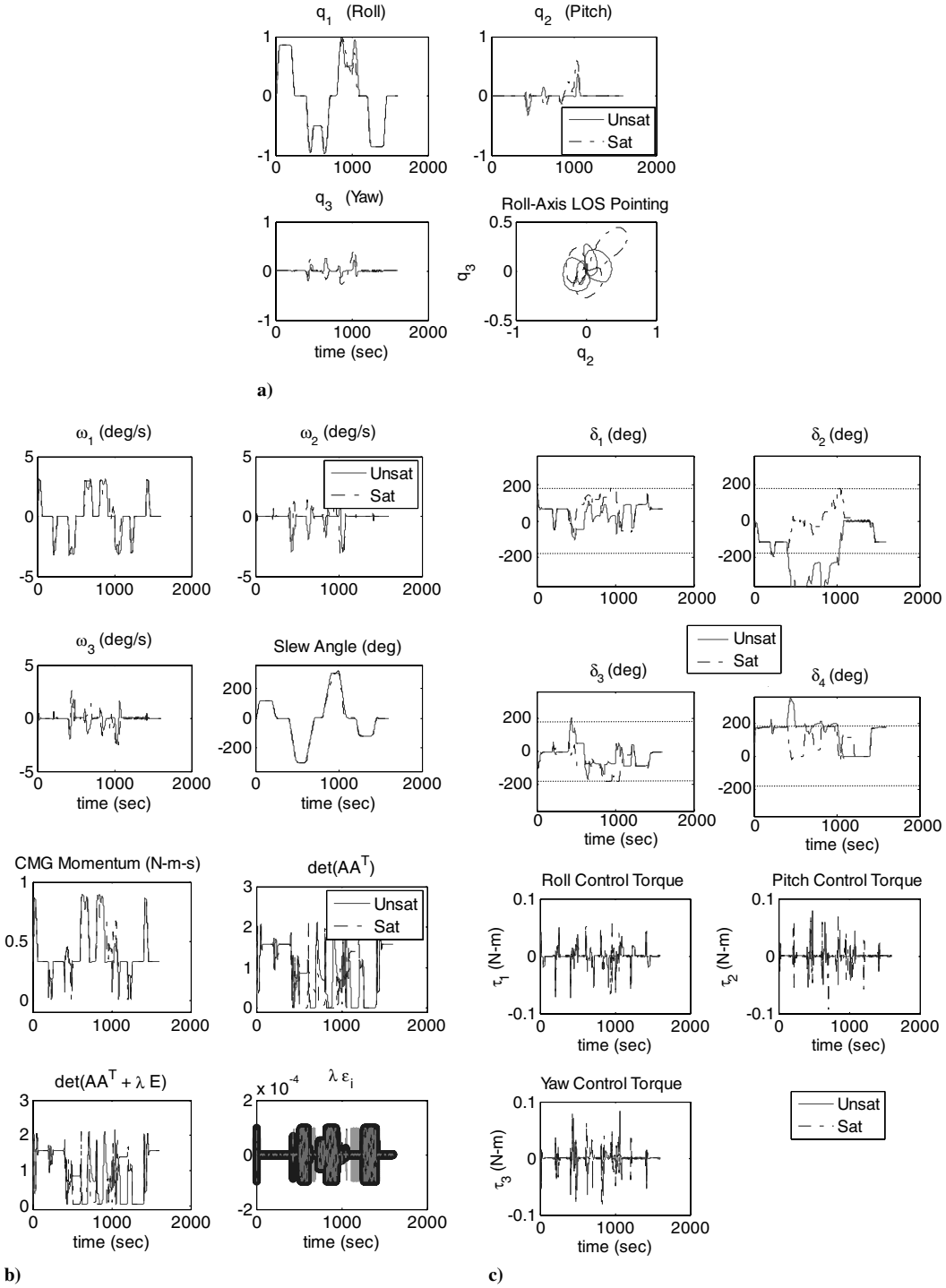

Fig. 6 Multiple maneuver profile with and without gimbal constraints.

which includes the required control torque, is used to generate the required gimbal angle profiles (gimbal rates); 2) the second part uses null motion to redistribute the gimbal angles to a preferred set of gimbal angles. The constant γ is used as a weighting factor into which task is implemented and with what weight. Selection of the weighting constant γ is based on trial and error for multiple case studies. Because of the CMG system constraints, it might not be able to achieve the preferred set of gimbal angles, however, the main task is to prevent the gimbal angles from going to the ± 180 deg constraint. Using the second null motion term is possible because the torque to produce term $\gamma[\,\mathbf{I} - \mathbf{A}^{\#} \quad \mathbf{A}\,][\boldsymbol{\delta}^* - \boldsymbol{\delta}]$ is always zero, due to the properties of null motion [7]. Figure 3 shows the new robust steering logic implemented on the single axis rest-to-rest 106 deg roll maneuver. Gimbal angles 2 and 4 time histories show the gimbal profile reaching the ± 180 deg constraint and then diverging away. Figures 4 and 5 show a similar example for a single axis roll rest-to-rest 180 maneuver. Gimbal angles 2 and 4 reach the 180 deg constraint and then diverge, however, due to the elliptic singularity, they are not completely prevented from reaching the ± 180 deg constraint.

Simulation Results

To evaluate the efficacy of the proposed gimbal-constrained CMG steering logic, an aggressive satellite slewing profile forcing the gimbals toward the constraints is needed. To this end, a series of realistic rest-to-rest, satellite roll maneuvers was simulated for both the unconstrained (unsaturated) and the constrained (saturated)

cases. Key parameters for the simulated maneuvers, which use the BILSAT-1 CMG, are shown in Fig. 1 and Table 1, whereas graphical results are given in Fig. 6. Note that the set of results figures contains plots of the constrained gimbal angle case (the dashed lines) superimposed upon the unconstrained gimbal angle case (the straight lines).

As shown in Figs. 6a and 6b, the maneuver profile calls for an out-and-return, rest-to-rest roll maneuver of 120 deg (without loss of generality, a maneuver starting from 0 deg roll, 0 deg pitch, and 0 deg yaw attitude), followed by similar out-and-return, rest-to-rest roll maneuvers of -300, $+300$, and -120 deg, all starting from 0 deg in satellite roll, pitch, and yaw configurations. In addition, Fig. 6b of this figure shows the satellite angular velocity profile during the maneuver. Figure 6b shows the roll, pitch, and yaw performance of the constrained and unconstrained cases as well as the roll line-of-site (LOS) error induced by the saturation control scheme (Fig. 6a). Here, both cases follow the desired slew angle quite well, but, around 1000 s, the gimbal constraint takes its toll in roll off-axis pointing error, which is recovered later in the maneuver. Notice the slight errors in pitch and yaw around 1000 s which then contribute to the larger LOS error for the unsaturated and saturated control. These errors are most likely due to the double-hump peaks during the -300 and the 300 deg maneuvers. This follows from taking the sine of angles from -240 to -300 deg and back to -240 deg as the sine value decreases from -240 to -270, then climbs from -270 to -300, briefly levels out, then decreases and climbs from -300 to -270 to -240 to 0. A similar phenomenon occurs from 0 to 300 back to 0 deg.

The CMG actuator response to this aggressive slewing profile is first seen in the gimbal angle history shown in Fig. 6c. As one can see, the gimbals start from a worst-case elliptic singularity ($[90 \quad 0 \quad -90 \quad 0]$ deg) and are required to exceed their ± 180 deg stop. It is clear that the satellite with saturated gimbal angles, when implementing the prescribed CMG steering logic, will be able to maintain the desired pointing, albeit with error until the steering logic controller recovers. Figure 6c shows the associated gimbal rates driving each CMG to achieve the maneuver, while it also shows the resulting torque produced by each CMG. These plots show similar shapes from both the torque and the gimbal rate data. This helps illustrate the concept that conventional CMG torque follows the gimbal rates from gimbal rate commanding of velocity-base CMG steering logic. The defined steering logic parameters are presented in Fig. 6b. The figure shows that the CMG momentum is similar in both cases, except around the same 1000 s portion as before. Similarly, the other plots also show this dropout around 1000 s. Thus, one can see that the desired, aggressive slewing profile can be achieved with constrained CMGs using the saturation CMG steering logic, but the drawbacks are that LOS error (for a roll maneuver) gets sightly worse than in the nonsaturation control law case; torque production and achievable gimbal rates change as the gimbals find new sets of angles to reach. Nevertheless, the presented CMG gimbal constraint steering logic algorithm permits achieving the desired attitude/attitude profile (i.e., the heart of the LOS plot) in finite time, while only trading off vanishing line-of-site error.

Conclusions

A mechanical gimbal angle constraint significantly simplifies the design of control moment gyroscopes. A robust CMG steering logic has been presented in which singularities can be escaped with gimbal constraints successfully. Worst-case scenarios, such as starting a maneuver within an elliptic singularity, show that the proposed control logic steers gimbal angles away from its hard 180 deg constraint.

References

[1] Gomes, L., Yuksel, G., Lappas, V., da Silva Curiel, B. A., Ozkaptan C., and Sweeting, M., "BILSAT-1: Advancing Smallsat Capabilities," AIAA SSC03-VI-4, Aug. 2003.

[2] Defendini, A., Lagadec, K., Guay, P., Blais, T., and Griseri, G., "Low Cost CMG-Based AOCS Designs," ESA, Noordwijk, The Netherlands, 2000, pp. 393–398.

[3] Lappas, V. J., "A CMG Based ACS System for Agile Small Satellites," Ph.D. Dissertation, Univ. of Surrey, Guildford, U.K., October 2002.

[4] Wie, B., *Space Vehicle Dynamics and Control*, AIAA Education Series, AIAA, Reston, VA, 1998, Chap. 7.

[5] Wie, B., Heiberg, C., and Bailey, D., "Singularity Robust Steering Logic for Redundant Single-Gimbal Control Moment Gyros," *Journal of Guidance, Control, and Dynamics*, Vol. 24, No. 5, 2001, pp. 865–872.
doi:10.2514/2.4799

[6] Wie, B., Heiberg, C., and Bailey, D., "Rapid Multi-Target Acquisition and Pointing Control of Agile Spacecraft," *Journal of Guidance, Control, and Dynamics*, Vol. 25, No. 1, 2002, pp. 96–104.
doi:10.2514/2.4854

[7] Vadali, S. R., Oh, H. S., and Walker, S. R., "Preferred Gimbal Angles for Single Gimbal Control Moment Gyros," *Journal of Guidance, Control, and Dynamics*, Vol. 13, No. 6, 1990, pp. 1090–1095.
doi:10.2514/3.20583